

Remotely Triggered Seismicity on the United States West Coast following the M_w 7.9 Denali Fault Earthquake

by S. G. Prejean, D. P. Hill, E. E. Brodsky, S. E. Hough, M. J. S. Johnston, S. D. Malone, D. H. Oppenheimer, A. M. Pitt, and K. B. Richards-Dinger

Abstract The M_w 7.9 Denali fault earthquake in central Alaska of 3 November 2002 triggered earthquakes across western North America at epicentral distances of up to at least 3660 km. We describe the spatial and temporal development of triggered activity in California and the Pacific Northwest, focusing on Mount Rainier, the Geysers geothermal field, the Long Valley caldera, and the Coso geothermal field.

The onset of triggered seismicity at each of these areas began during the Love and Raleigh waves of the M_w 7.9 wave train, which had dominant periods of 15 to 40 sec, indicating that earthquakes were triggered locally by dynamic stress changes due to low-frequency surface wave arrivals. Swarms during the wave train continued for ~ 4 min (Mount Rainier) to ~ 40 min (the Geysers) after the surface wave arrivals and were characterized by spasmodic bursts of small ($M \leq 2.5$) earthquakes. Dynamic stresses within the surface wave train at the time of the first triggered earthquakes ranged from 0.01 MPa (Coso) to 0.09 MPa (Mount Rainier). In addition to the swarms that began during the surface wave arrivals, Long Valley caldera and Mount Rainier experienced unusually large seismic swarms hours to days after the Denali fault earthquake. These swarms seem to represent a delayed response to the Denali fault earthquake. The occurrence of spatially and temporally distinct swarms of triggered seismicity at the same site suggests that earthquakes may be triggered by more than one physical process.

Introduction

The onset of remotely triggered seismicity across the western United States immediately after the 1992 M_w 7.3 Landers earthquake (Hill *et al.*, 1993; Anderson *et al.*, 1994; Hill *et al.*, 1995) surprised many Earth scientists and raised many intriguing questions about the physical processes that initiate earthquakes. Static stress changes from the Landers rupture dropped below tidal stresses at distances beyond 300 km and were thus too small to explain the triggered seismicity observed at distances from 400 km to as great as 1250 km (Hill *et al.*, 1993). Since Landers, similar episodes of remotely triggered seismicity have been documented in the western United States and Mexico after the 1999 M_w 7.1 Hector Mine, California earthquake (Gomberg *et al.*, 2001; Glowacka *et al.*, 2002); in Katmai National Park, Alaska, after the 1999 M_w 7.0 Karluk Lake earthquake and the 2000 M_w 6.9 Kodiak Island earthquake (Power *et al.*, 2001; Moran *et al.*, 2004); in Greece after the 2000 M_w 7.4 Izmit, Turkey, earthquake (Brodsky *et al.*, 2000); and in the Geysers geothermal area in northern California after several large earthquakes (Stark and Davis, 1996). These studies provide strong evidence that earthquakes are initiated dynamically during the passage of seismic waves from both local earth-

quakes (Gomberg *et al.*, 2003) and large distant earthquakes (e.g., Hill *et al.*, 1993; Gomberg *et al.*, 2001, 2004).

Based on these observations, researchers have proposed many intriguing explanations of the physical processes that lead to remotely triggered seismicity. Because of limitations in available data, however, we are just beginning to understand the characteristics of triggered seismicity and cannot yet rule out any of these models. One impediment to deciphering the physical processes producing remotely triggered seismicity has been a poor understanding of the true spatial and temporal distribution of triggered events after large earthquakes due to limitations in seismometer distribution, bandwidth, and dynamic range and limitations of catalogs that are incomplete at small magnitudes.

The M_w 7.9 Denali fault earthquake of 3 November 2002, which triggered bursts of local earthquakes across western North America at epicentral distances of up to at least 3660 km (Fig. 1), provided one of the most impressive and best recorded examples of remotely triggered seismicity yet observed. In this article we describe the spatial and temporal distribution of remotely triggered seismicity in California and the Pacific Northwest. We interpret these obser-

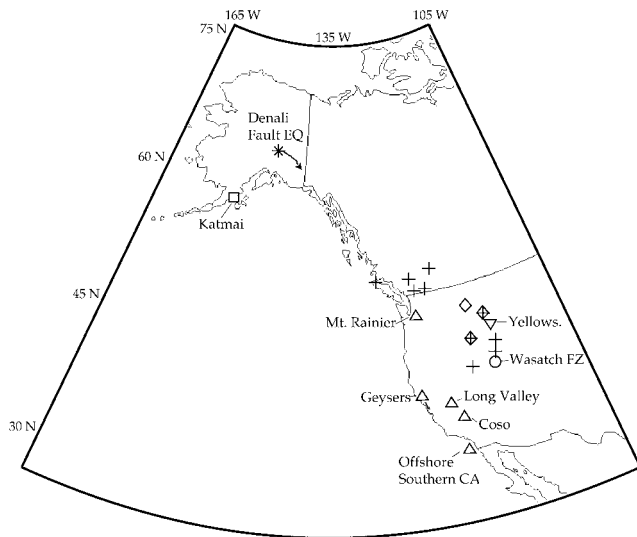


Figure 1. Map of North America showing location of Denali fault earthquake (star) and locations where remotely triggered seismicity was observed in response to the Denali fault earthquake. Triangles are areas discussed in this study. Square, Moran *et al.* (2004); diamonds, Husker and Brodsky (2004); inverted triangle, Husen *et al.* (2004); circle, Pankow *et al.* (2004); plus signs (Gomberg *et al.*, 2004). The dashed line denotes the strike of the Denali-Totschunda fault. Arrow indicates direction of rupture.

vations in the context of triggered seismicity observed after previous large earthquakes to explore characteristics of remotely triggered seismicity and investigate the nature of this phenomenon.

Seismicity Triggered Remotely by the Denali Fault Earthquake

The 2002 Denali fault earthquake was among the largest continental earthquakes recorded in the United States. Its epicenter was located about 65 km east of Denali National Park and 270 km north of Anchorage, Alaska (Fig. 1). Waveform modeling indicates that the earthquake began as a deep thrust rupture on the previously unknown Susitna Glacier fault (Eberhart-Phillips *et al.*, 2003). It subsequently ruptured the Denali fault unilaterally from west to east and the Totschunda fault to the southeast in a right lateral sense with a maximum surface rupture of 8.8 m.

We use two methods to investigate whether the Denali fault earthquake triggered local earthquakes in California and the Pacific Northwest. First, to search for triggered seismicity in earthquake catalogs for the regions monitored by the Southern California (SCSN) and Northern California Seismic Networks (NCSN), we used the beta statistic approach of Matthews and Reasenber (1988) to compare seismic activity during the month before and the month after the Denali fault mainshock. These calculations reveal some regions of positive seismicity increase in both northern and

southern California. However, comparing these rate changes with the changes observed from any given month of seismicity to the next, we conclude that the pre- versus post-Denali fault activity reveals no evidence for significant seismicity rate changes. Similarly, examining the earthquake catalog from the Pacific Northwest Seismic Network (PNSN) in time slices before and after the Denali fault earthquake shows no significant seismicity rate change over the region including western Oregon and Washington. Thus, based on catalogs alone, it would appear that no earthquakes were triggered in California or the Pacific Northwest.

As a second approach, we high-pass-filtered broadband and strong-motion recordings of the mainshock wave train to look for small local earthquakes hidden in the surface wave arrivals and early coda that are not in earthquake catalogs. For this analysis we examined all broadband waveforms from the SCSN, NCSN, and PNSN. We visually compared 1-hr time windows before and after the mainshock arrival time. We identified hundreds of small earthquakes that were not in earthquake catalogs at Mount Rainier in central Washington, the Geysers geothermal field in northern California, the Mammoth Mountain in eastern California, the Coso geothermal field in southeastern California, and offshore southern California (Fig. 1). We found no evidence for triggering at any other sites examined.

Mount Rainier

Mount Rainier, in the central Washington Cascades, responded to the Denali fault earthquake with a burst of six to eight small ($M = -2$ to $M = 0$) earthquakes during the highest-amplitude Love and Rayleigh wave arrivals from the mainshock (Fig. 2c,d; Table 1). The first triggered earthquake occurred at 22:25 coordinated universal time (UTC) 3 November, when ground shaking from the Denali fault earthquake reached its peak amplitude at Rainier. The dynamic stress at the time of the first earthquake was roughly 0.09 MPa (dynamic stress changes calculated following Hill *et al.*, 1993). These earthquakes were clearly recorded only by the broadband/strong-motion station on Mount Rainier (station LON of the PNSN), so it was not possible to locate them. Thus, none of the earthquakes triggered during the mainshock surface waves are in the PNSN catalog.

A second swarm containing about eight earthquakes began 2.5 hr later (between 00:55 and 03:30 UTC on 4 November) (Fig. 2a). Unlike the initial swarm, these earthquakes were well recorded on enough low-dynamic-range stations to be located ($M \sim -1.2$ to $M \sim 0.9$) and appear in the PNSN catalog. They occurred directly beneath the summit of the mountain near the base of the volcanic edifice (~ 0 – 2 km above sea level) over an area with a diameter of 4 km. These locations are typical of background seismicity for the volcano (Moran *et al.*, 2000). Because the waveforms on the broadband station of these later earthquakes were similar to those of the initial swarm, it is likely that the earlier swarm occurred in the same crustal volume.

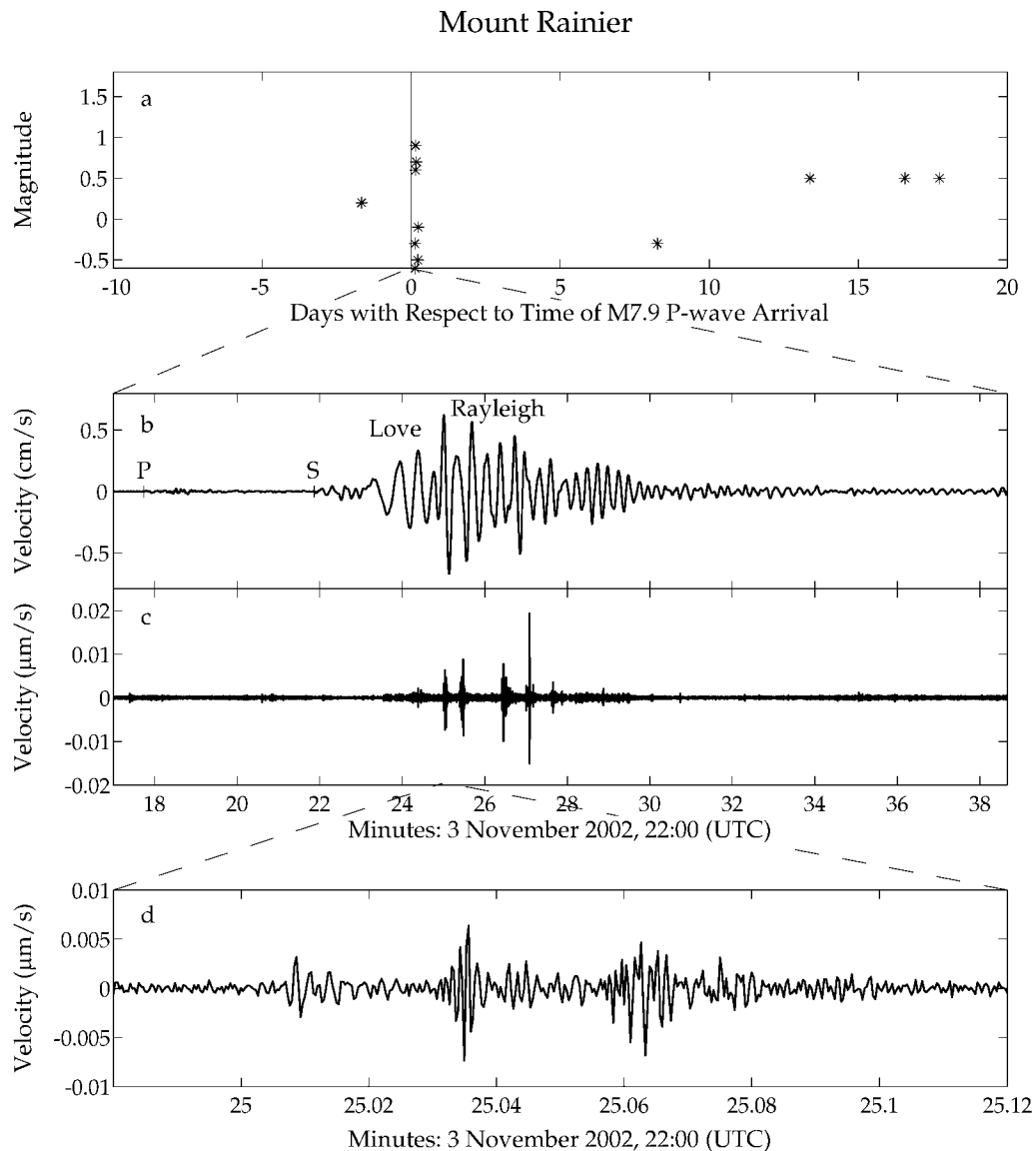


Figure 2. Seismicity triggered at Mount Rainier. (a) Catalog from PNSN, showing a small swarm beginning 2.5 hr after the Denali fault earthquake wave train passed through the area. All other panels show data from a very small swarm that was triggered during the passing waves from the Denali fault earthquake; these earthquakes are not in the PNSN catalog. (b) Broadband waveform from station LON, north component, showing the Denali fault earthquake wave train at Rainier. Major arrivals are labeled. We did not rotate LON records into ray coordinates because other components are clipped. (c) Record from b high-pass-filtered, showing small local earthquakes occurring during Denali fault earthquake wave train. (d) Detail of record from c, showing swarm-like character of triggered events.

Although the response of Mount Rainier to the Denali fault earthquake was weak relative to some other sites discussed in this article, the triggered swarms were unusually vigorous compared with the volcano's background seismicity. Mount Rainier usually has only one to two small earthquakes per month. Although Mount Rainier is situated in a compressional tectonic environment, normal faulting focal mechanisms are commonly observed for shallow earthquakes located directly beneath the volcano, consistent with

an extensional stress state in the vicinity of the triggered earthquakes (Giampiccolo *et al.*, 1999). Based on focal mechanisms, seismic tomography, and geochemical studies, Moran *et al.* (2000) infer that earthquakes in this location typically occur in response to the movement of magmatically derived fluids through the volcano's edifice.

Mount Rainier was the only Cascade volcano observed to respond to the Denali fault earthquake. However, it is the only Cascade volcano with a high-dynamic-range instrument

Table 1
Summary of Remotely Triggered Seismicity

Site	Distance (km)	Az	Seismicity Triggered during and Minutes after Denali Fault Earthquake Wave Train								Swarms Delayed by Hours to Days			
			Onset (min)	N_H	N_L	N_R	M_{max}	Duration (min)	S_{onset} (MPa)	S_{max} (MPa)	Onset (hr)	N	M_{max}	Duration
Mt. Rainier, WA	3108	127°	12.64	6–8	—	0	0.0	6	0.09	0.9	2.5	8 (N_H)	0.9	3 hr
Geysers, CA	3120	137°	12.22	100	64	19	2.5	40	0.03	0.07	—	—	—	—
Mammoth, Long Valley, CA	3454	133°	17.20	60	0	0	0.8	15	0.03	0.06	23.5	112 (N_R)	3.0	17 days
Coso, CA	3660	132°	15.07	—	80	1	2.3	20	0.01	0.03	—	—	—	—
Offshore southern california	4003	135°	—	2	0	0	2.5	—	—	0.02	—	—	—	—

Distance and azimuth with respect to the Denali fault earthquake epicenter (63.520 N, -147.530 W). Onset is the delay from the origin time of the Denali fault earthquake (22:12:41 UTC) to the first locally triggered earthquake. N is approximate number of triggered earthquakes; N_H were counted by hand on one station; N_L were detected and located by dense local networks; N_R were detected and located by regional networks; M_{max} is magnitude of the largest triggered earthquake; S_{max} is the estimated peak dynamic stress for the seismic waves from the Denali fault earthquake; S_{onset} is the estimated dynamic stress at the time of the first triggered earthquake for earthquakes triggered before largest surface wave arrivals. Dynamic stress calculations follow Hill *et al.* (1993).

close by. It is possible that other Cascade volcanos had triggered events during the passage of the large-amplitude surface waves, which saturated all local monitoring stations, although none of them had unusual earthquakes after the surface waves when seismograms were back on-scale. Notably, several Cascade volcanos (Mount Lassen, Mount Shasta, and Medicine Lake) experienced triggered seismicity after the 1992 Landers earthquake, but Mount Rainier did not. Triggered seismicity was also not observed at Mount Rainier after the M_w 6.8 Nisqually Benioff zone earthquake of 28 February 2001, 82 km west of Mount Rainier and 52 km deep.

Geysers Geothermal Field

The Geysers geothermal field, in northern California, responded energetically to the Denali fault earthquake, producing roughly 100 earthquakes in spasmodic bursts between 22:25 and 22:48 UTC 3 November (Fig. 3b, Table 1). We hand counted these earthquakes at NCSN short-period station GDX. The NCSN regional seismic network identified and located 19 of these earthquakes, whereas the locally dense Calpine Geysers Seismic Network, which consists of 22 stations over an area of 50 km², identified and located 64 earthquakes. This relatively strong but brief response resembled the Geysers response to seven other remote western North America earthquakes (Stark and Davis, 1996), including Landers. The triggered seismicity began immediately after arrival of the first Love wave, when the estimated dynamic stress was only 0.03 MPa. The largest earthquakes, however, including four M 2 and greater events based on the Northern California Earthquake Data Center (NCEDC) catalog, did not occur until 3–13 min after the initial arrival of the Rayleigh waves, well after the Love wave train (Fig. 3). Peak dynamic stresses were 0.07 MPa during the Rayleigh waves. Seismicity rates decreased rapidly after the largest surface waves had passed. No delayed earthquakes occurred at the Geysers.

Epicenters determined by the dense Calpine network were scattered throughout the ~ 10 km by 20 km area that is typically active in the Geysers area, similar to the Coso geothermal field (see below). Depths ranged from 0 to 6 km. These earthquake location and magnitude distributions are similar to those observed for swarms during previous episodes of triggering. Although the Geysers geothermal field is located within the transpressional San Andreas fault system, the region is an area of local crustal extension (Weaver and Hill, 1978/79).

Mammoth Mountain and the Long Valley Caldera

The Long Valley caldera is located in eastern California on the western border of the actively extending Basin and Range province. Mammoth Mountain, a 50,000-year-old volcano located near the southwest rim of the caldera (Bailey, 1989), responded to the Denali fault earthquake with a burst of roughly 60 small earthquakes ($M \leq 0.8$) that began at 22:29:51 UTC on 3 November during the largest amplitude Rayleigh waves from the Denali fault earthquake wave train (Fig. 4, Table 1). The earthquakes triggered during the surface wave arrivals were best recorded on University of Nevada, Reno/USGS station OMM, located off the southeastern flank of Mammoth Mountain (Fig. 5). The triggered swarm continued for 15 min. The seismicity rate was highest during the largest-amplitude Rayleigh waves, which had peak dynamic stresses of 0.06 MPa. Seismicity died out rapidly after the surface waves passed.

None of these earthquakes were identified and located by standard network processing, although one event was large enough to be located by hand in postprocessing. This earthquake occurred beneath the south flank of Mammoth Mountain near Horseshoe Lake at ~ 2.5 km depth. Because the waveforms and S - P times for the smaller triggered earthquakes were similar to the one that could be located, it is likely that all 60 occurred in approximately the same location.

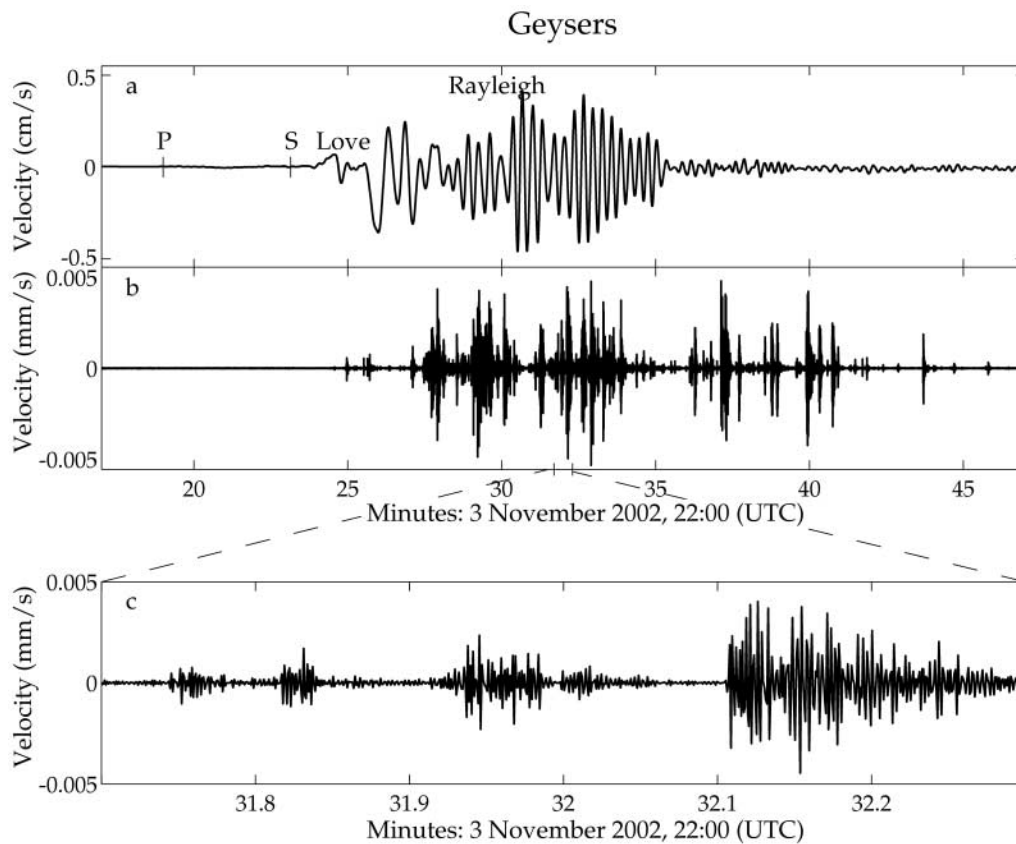


Figure 3. Seismicity triggered at the Geysers. (a) Broadband waveform from NCSN station HOPS (10 km north of the Geysers) rotated to transverse direction, showing Denali fault earthquake wave train in the Geysers area. Major arrivals are labeled. (b) Short-period record from GDX, high-pass-filtered, showing small local earthquakes occurring during Denali fault earthquake wave train. (c) Detail of record from b showing swarm-like character of triggered events.

Whether the single small earthquake coincident with the *S*-wave arrival (Fig. 4d) was a triggered event or simply a coincidental background earthquake is unclear. This earthquake was located 10 km to the east of the swarm triggered during the surface waves in the caldera's south moat, an area that had elevated seismicity in the weeks before the Denali fault earthquake.

The triggered seismicity at Mammoth Mountain coincided with a strain change during the Denali Fault earthquake Love wave arrivals detected on three borehole dilatometers near Mammoth Mountain (Johnston *et al.*, 2004) and a 13-cm water level drop that was followed by a gradual recovery in the 3-km-deep LVEW well in the center of Long Valley caldera. As for the previous two instances of remotely triggered seismicity in Long Valley caldera (Landers and Hector Mine), the strain change was much larger than can be accounted for by the cumulative slip associated with the triggered earthquakes (Johnston *et al.*, 2004).

At 21:38 UTC on 4 November, 23.5 hr after the triggered swarm under Mammoth Mountain, an earthquake swarm began in the south moat of the Long Valley caldera at 2–3 km depth. These earthquakes were located ~10 km

east of the earlier swarm beneath Mammoth Mountain and appear to be a delayed response to the Denali fault earthquake (Fig. 4a). This was the largest swarm in the Long Valley caldera in the past 4 years. In the 17-day-long swarm, 112 earthquakes were located by the network by using standard event detection and location algorithms. The swarm had a total seismic moment of 1.6×10^{14} N m and included nine $M > 2$ earthquakes, the largest of which was a $M 3$ earthquake at 04:08 UTC on 5 November.

To test the hypothesis that this swarm was triggered by the Denali fault earthquake, we used the NCEDC catalog from 1985 through 2003 to determine the likelihood of a $M 3$ earthquake occurring by random chance anywhere in the Long Valley caldera. The odds of seeing one $M 3$ + earthquake on any given day are about 2%. This is a conservative estimate, because the seismicity rate in Long Valley has been unusually low since 1999. Thus, there is a reasonable probability that the $M 3$ was triggered by the Denali fault mainshock.

The swarm triggered in the caldera's south moat was unusual in that (1) it occurred in a relatively aseismic section of the south moat, (2) focal depths of the swarm earthquakes

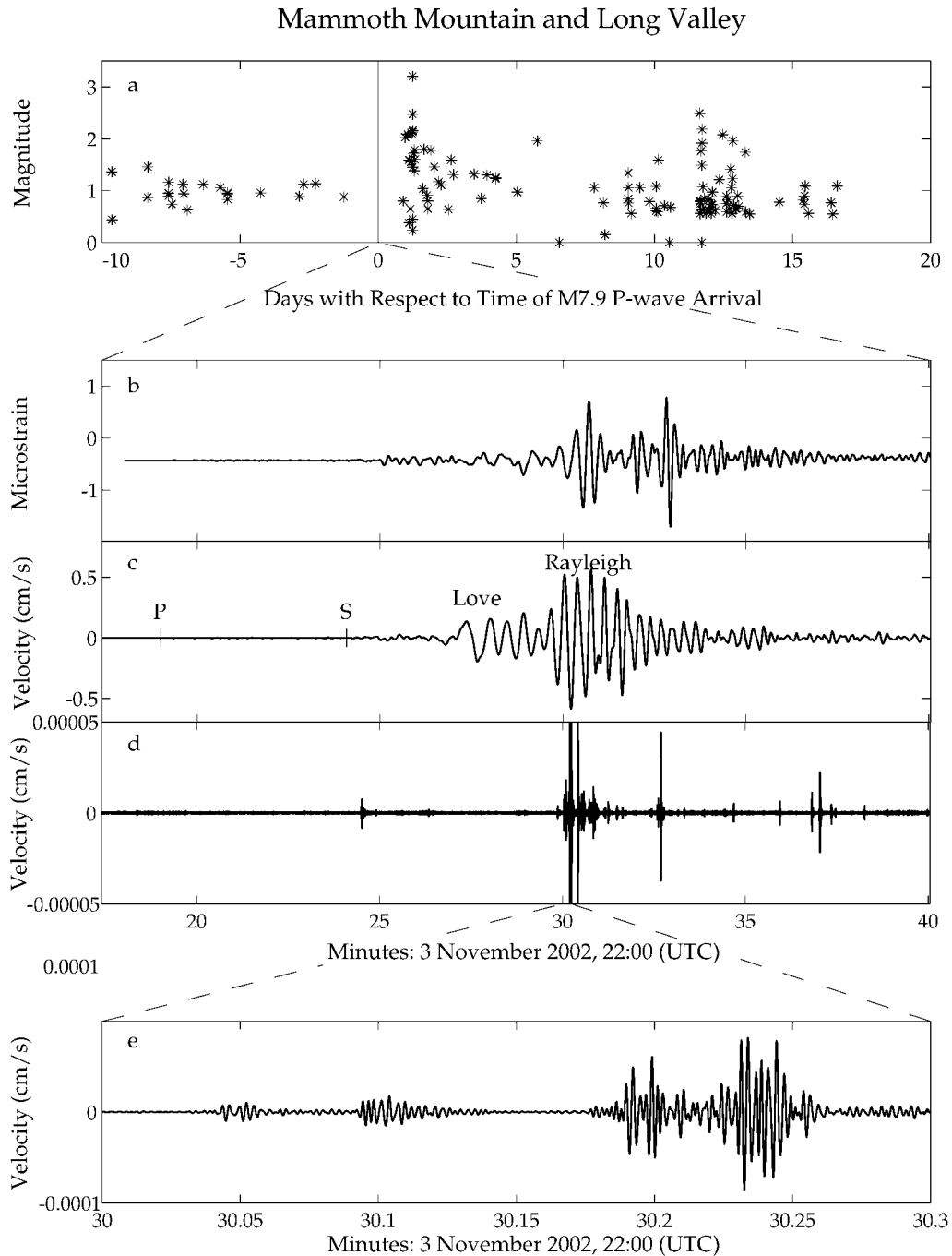


Figure 4. Seismicity triggered at Mammoth Mountain (d–e) and within the Long Valley caldera (a). (a) Catalog from NCEDC showing two swarms following the Denali fault earthquake in the caldera’s south moat. All other panels show data from a very small swarm at Mammoth Mountain that was triggered during the passing waves from the Denali fault earthquake; these earthquakes are not in the NCEDC catalog. (b) Motorcross strain meter record from Denali earthquake with coseismic signature and tides removed. (c) Broadband waveform from UNR/USGS station OMM rotated to transverse direction, showing Denali fault earthquake wave train at Long Valley. Major arrivals are labeled. (d) Record from c high-pass-filtered, showing small local earthquakes occurring during Denali fault earthquake wave train. (e) Detail of record from d, showing swarm-like character of triggered events.

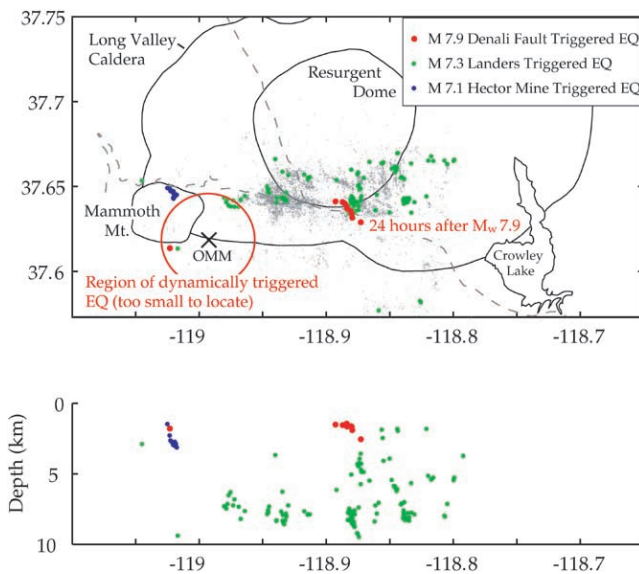


Figure 5. Map and east-west cross section of Long Valley area, showing hypocenters relocated by using HypoDD (Waldhauser and Ellsworth, 2000) for Landers (green), Hector Mine (blue), and the Denali fault earthquakes (red). 1997–1998 seismicity is shown in gray, for reference. The red circle around station OMM shows the epicentral area in which all earthquakes triggered during the mainshock's wave train must be located based on *S-P* times. However, it is likely that all earthquakes occurred in roughly the same location as the one we were able to locate.

were unusually shallow (<4 km depth), and (3) the north-northwest lineation of the swarm epicenters cut across the prevailing west-northwest trend of the usual south moat swarm activity (as did the seismicity triggered by Landers). This south moat swarm, however, does not appear to be accompanied by either a detectable strain change or significant changes in local water well levels. Seismicity rates in the south moat of the caldera remained unusually high for 17 days after the Denali fault earthquake with respect to background levels during the past 4 years.

The triggered response at Mammoth Mountain and within the Long Valley caldera varied significantly between the Landers, Hector Mine, and Denali fault earthquakes. The seismicity triggered by Landers (cumulative seismic moment 8.1×10^{14} N m), whose wave train had an estimated peak dynamic stress of ~ 0.3 MPa in the Long Valley area, was stronger and more extensive than the seismicity triggered by either the Hector Mine or Denali fault earthquakes, with peak dynamic stresses of 0.25 MPa and 0.06 MPa, and triggered seismic moments of 3.8×10^{12} N m and 1.6×10^{14} N m, respectively. In general, locations of earthquakes triggered by Landers, Hector Mine, and the Denali fault earthquake are similar, but vary in detail (Fig. 5). Most earthquakes triggered in the Long Valley area by the Landers earthquake occurred in the caldera's south moat, although at

significantly greater depths than those triggered there by the Denali fault earthquake. At least one earthquake triggered by Landers occurred in the Horseshoe Lake area. Hector Mine triggered earthquakes in the Mammoth Mountain region as well, but these occurred under the mountain's north flank.

Coso Geothermal Field

The Coso geothermal field is located at the southern end of the Owens Valley in a transtensional tectonic regime (Unruh *et al.*, 2002), 3660 km southeast of the Denali fault earthquake epicenter. A burst of ~ 80 small earthquakes was identified by the Coso Micro-Earthquake Network. The first and largest of the triggered earthquakes coincided with the onset of the Love wave arrival at 22:28 UTC, when the estimated dynamic stress was ~ 0.01 MPa (Fig. 6, Table 1). The first earthquake had a magnitude of M 2.3. Of all the triggered earthquakes at Coso, this event alone appeared in the Southern California Earthquake Data Center (SCEDC) catalog. Approximately 200 sec after this earthquake, during the largest-amplitude Rayleigh wave arrivals (peak dynamic stress of ~ 0.03 MPa), a swarm of triggered earthquakes occurred as a spasmodic bursts sequence ($M \leq 0.5$). Activity gradually died out within 20 min of the swarm's onset.

Earthquakes large enough to be located were scattered throughout the $\sim 10 \times 10$ km area of recurring earthquake swarm activity in the geothermal field. Their depths ranged from 0.05 to 3.5 km. This spatial distribution is unusual for the Coso area, because swarms usually occur in isolated clusters, rather than scattered throughout the entire field. Remotely triggered seismicity was observed previously at Coso after the Landers earthquake (Hill *et al.*, 1993). In this study, we also identified triggered seismicity due to the Hector Mine earthquake by reanalyzing data and high-pass-filtering broadband waveforms. Coso's response to Landers, which had a peak dynamic stress of 0.5 MPa, was stronger than its Denali fault earthquake response. In Landers 44 triggered earthquakes were located by the regional network, including a M 4.4 event (Hill *et al.*, 1993). Coso's response to the Hector Mine earthquake, which had a peak dynamic stress of 0.1 MPa, was considerably weaker than either the Landers or the Denali fault earthquake response. The Hector Mine earthquake response consisted of only 26 triggered earthquakes, all too small to be located by the locally dense Coso Micro-Earthquake Network.

Offshore Southern California

By examining broadband seismograms throughout southern California, we identified two earthquakes in the early coda of the Denali fault earthquake wave train that had escaped routine network analysis. Although we cannot rule out the possibility that these earthquakes occurred by chance, we explore the possibility that they were triggered

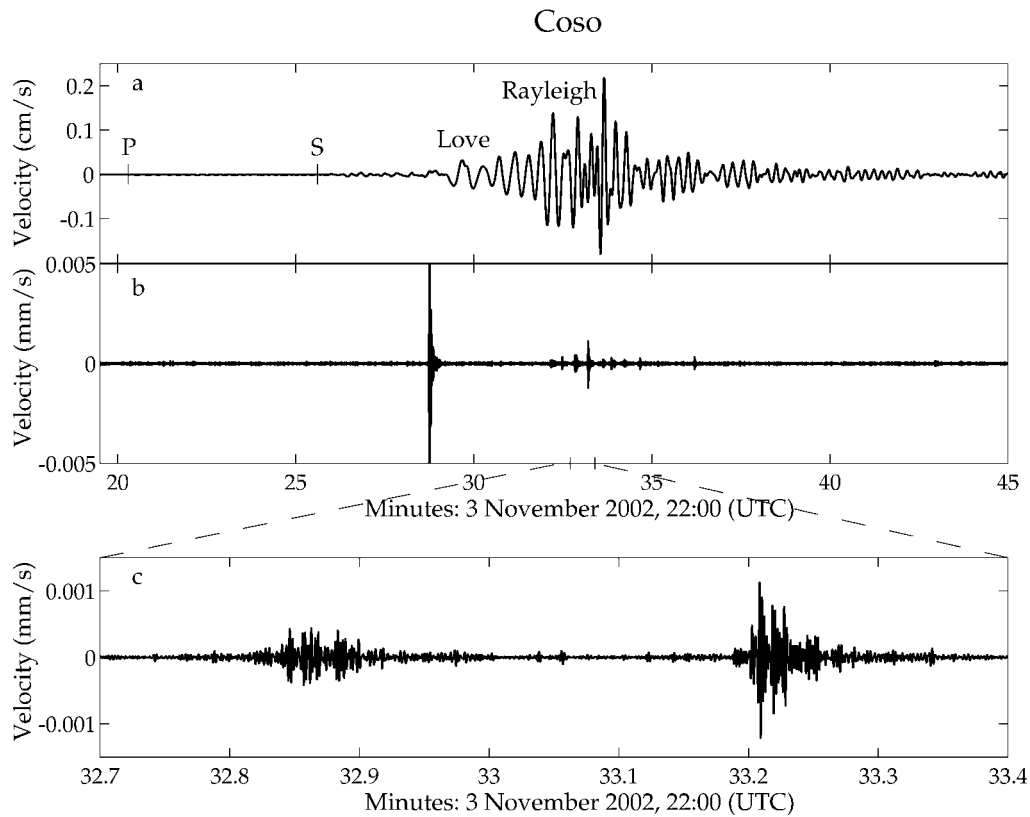


Figure 6. Seismicity triggered at Coso. (a) Broadband wave form from SCSN station JRC rotated to transverse direction, showing Denali fault earthquake wave train in Coso area. Major arrivals are labeled. (b) JRC record high-pass-filtered, showing small local earthquakes occurring during Denali wave train. (c) Detail of record from b, showing swarm-like character of triggered events.

and discuss the implications. Using standard network analysis of filtered recordings of the second and larger of these events, we obtained a local magnitude estimate of 2.5 and a location approximately 125 km offshore of southern California (Fig. 1, Table 1). The first event could not be located but appears to have had a similar source location and a magnitude of approximately 1.8. Located 4003 km from the Denali fault earthquake epicenter, this may be the most distant example of remotely triggered seismicity yet documented.

Because it is much more difficult to determine whether single earthquakes were triggered by a large distant earthquake, in contrast to the swarms discussed earlier, we used the SCEDC catalog to determine the likelihood of a M 2.5 earthquake occurring by random chance anywhere in the region monitored by the SCSN. The odds of seeing one M 2.5+ event in any given hour is approximately 8%. Based on this criterion, we can reject the hypothesis that this earthquake occurred by chance at the 90% confidence level. This is a conservative estimate, because the offshore California seismicity rate is low compared with most of the area monitored by the SCSN. Thus, there is a reasonable probability that the larger of the offshore events was triggered by the Denali fault mainshock. The evidence for triggering in this

case is considerably weaker than for the other sites discussed in this study. The offshore California case highlights the difficulties associated with identifying triggered earthquakes that do not occur in swarms in well-instrumented areas.

Summary of Observations

In each of the areas considered here, the onset of locally triggered seismicity began as the Love and Rayleigh surface waves from the Denali fault earthquake propagated through the area with estimated dynamic stress changes as small as 0.01 MPa. The onset of the triggered response began at the time of the initial Love wave arrival (the Coso and Geysers geothermal fields), during the Rayleigh wave arrivals (Mount Rainier and Mammoth Mountain), or during the coda (offshore southern California). At the four volcanic/geothermal sites, the local earthquakes that were triggered during the wave train of the mainshock developed as rapid-fire sequences of small ($M < 3$) earthquakes that persisted for several minutes in the case of Mount Rainier to 40 min in the case of the Geysers. Hill *et al.* (1990) note that earthquake swarms of this type (spasmodic bursts) are distinctly different in character from mainshock-aftershock earthquake

sequences and are commonly observed in geothermally or volcanically active environments. At all four volcanic/geothermal sites, seismicity rates were highest during the largest-amplitude surface waves, when strain rates reached their peak, and declined quickly once the surface waves passed.

In addition to the seismicity triggered during the Denali fault earthquake wave train, Mount Rainier and the Long Valley caldera exhibited increased seismicity levels in the days to weeks afterward that seem to represent a delayed response to the earthquake. Husen *et al.* (2004) document a delayed burst of apparently triggered seismicity at Yellowstone as well. In the case of Long Valley and Mount Rainier, these delayed swarms contained larger earthquakes than the initial swarms that occurred during the passage of the Denali fault earthquake wave train.

Discussion

The distribution of seismicity remotely triggered by the Denali fault earthquake in the conterminous western United States overlaps the areas triggered by the Landers and Hector Mine earthquakes. Although smaller, the epicenters of the Landers and Hector Mine earthquakes were closer to the sites at which triggering occurred (distances of 200 to 1200 km), and the dynamic stresses at many of the triggered sites were similar to or somewhat larger than those generated by the Denali fault earthquake (Hill *et al.*, 1993; Gomberg *et al.*, 2001). Sites that responded to both the Denali fault and Landers earthquakes include the Geysers, the Long Valley caldera region, the Coso geothermal field, Yellowstone (Husen *et al.*, 2004), Cascade, Idaho (Husker and Brodsky, 2004), and the southern section of the Wasatch fault zone near Cedar City, Utah (Pankow *et al.*, 2004). Sites that responded to both the Denali fault and Hector Mine earthquakes include the Geysers (Gomberg *et al.*, 2001), Mammoth Mountain, and Coso.

By comparing three episodes of triggered seismicity (Landers, Hector Mine, and Denali), we conclude that triggering occurs predictably in some places, specifically the Geysers (as shown by Gomberg and Davis, 1996), the Long Valley region, and Coso. This supports the idea that seismicity will be triggered at some sites if a site-specific threshold in amplitude and frequency of ground shaking exists (Anderson *et al.*, 1994; Gomberg and Davis, 1996; Gomberg *et al.*, 2001; Brodsky and Prejean, 2003; Moran *et al.*, 2004). That is, some areas do not appear to require any “recharge” time for triggering to recur. For example, episodes of triggered seismicity at the Geysers have been separated by times as short as 2 months (Stark and Davis, 1996). However, at other areas, such as the Cascade volcanoes, the response to distant large earthquakes may be less predictable. These sites highlight the fact that the dynamic stress threshold to initiate triggered activity may be time dependent in at least some regions.

With the exception of the Katmai volcanic cluster in

southern Alaska (Moran *et al.*, 2004), all the areas with a recognized triggered response to the Denali fault earthquake (this study; Husker and Brodsky, 2004; Pankow *et al.*, 2004; Husen *et al.*, 2004; Gomberg *et al.*, 2004) lie southeast of the mainshock epicenter and thus in the general direction of the mainshock rupture propagation (see Fig. 1). Because the rupture propagated toward the southeast, British Columbia and the western United States, in particular, western Montana, Wyoming, and Utah, were directly in line with the strike of the earthquake, and thus experienced pronounced rupture directivity effects from the teleseismic *S* waves and surface waves (Eberhart-Phillips *et al.*, 2003). Although several authors have observed a triggered response in the areas of maximum directivity (Husker and Brodsky, 2004; Pankow *et al.*, 2004; Gomberg *et al.*, 2004), the level and duration of triggered response does not seem to be simply a function of dynamic stress amplitude. Areas with the most vigorous triggered seismicity are Yellowstone ($M \leq 3.2$, ~ 600 earthquakes, 0.2-MPa dynamic stress) (Husen *et al.*, 2004), the Wasatch front in Utah ($M \leq 3.3$, 110 earthquakes, 0.2-MPa dynamic stress) (Pankow *et al.*, 2004), the Long Valley area ($M \leq 3.0$, ~ 200 earthquakes, 0.06-MPa dynamic stress). Thus, although earthquake triggering may occur in any tectonic environment (Gomberg *et al.*, 2004), it is likely that some regions are more susceptible to large-scale triggering than others.

Our impression of the distribution of remotely triggered earthquakes is no doubt colored by both the distribution of local monitoring networks and the apparent propensity of triggered seismicity to occur in swarms. Because most of the triggered earthquakes were small ($M < 1$) and occurred during the high-amplitude surface wave arrivals, they could only be identified by examining unclipped waveform data from stations located less than 10 km from the sites of remotely triggered activity. Thus, recently installed high-dynamic-range seismometers across the western United States allowed us to identify bursts of small, triggered earthquakes during the Denali fault earthquake wave train that would have gone unnoticed on the more common, low-dynamic-range instruments that saturate during large ground motions. Notably, of the hundreds of earthquakes identified in this study that were triggered within 30 min of the Denali fault earthquake, only 20 were detected by routine processing of data recorded by regional networks (Table 1).

In cases where triggered earthquakes were large enough to be detected by regional networks, the number of triggered events was too small to generate a rate increase that is statistically distinguishable from normal seismicity fluctuations. Even in the Coso region, where the local network provides compelling evidence for early triggered events, the rate increase is not significant with the beta statistic on the SCDEC catalog. Whether isolated earthquakes, such as the $M 2.5$ event offshore southern California, was in fact triggered by dynamic stresses from the Denali fault earthquake remains a question of statistical significance.

Physical Processes Leading to the Remote Triggering of Seismicity

Several researchers have proposed a range of physical processes that might generate remotely triggered earthquakes. One class of models attributes triggered seismicity to changes in crack conductivity and pore fluid pressure in the Earth's crust as the seismic waves from a large distant earthquake perturb a region's hydrothermal system and redistribute pore pressure (Hill *et al.*, 2002; Brodsky *et al.*, 2003). A second class of models involves changes in fluid pressure as bubbles oscillate or rise through fluid or fluid-saturated rock (Linde *et al.*, 1994; Brodsky *et al.*, 1998). A third class of models involves changes in the state of magma bodies triggered by dynamic stresses from a distant earthquake (Linde *et al.*, 1994; Hill *et al.*, 2002). A fourth class of models suggests that dynamic stresses from the mainshock change the state of a fault or the friction across a fault surface, leading to triggered earthquakes (Gomberg and Davis, 1996; Gomberg *et al.*, 1998, 2001; Gomberg, 2001; Hough and Kanamori, 2002; Voisin, 2002).

Observations described here show that triggered seismicity in volcanic and geothermal environments often occurs immediately after the arrival of the mainshock's surface waves with periods of >10 sec. Also, seismicity rates during the mainshock wave train are highest during the highest-amplitude arrivals with the highest peak strains (Fig. 4). This strongly suggests that seismicity triggered during the mainshock's wave train represents an almost instantaneous response to stress changes due to low-frequency wave arrivals. Thus, physical models that require a significant response time cannot explain earthquakes triggered so quickly (Table 2). This includes all models that rely on changes in deep magmatic systems to trigger seismicity and models that require fluids to move a significant distance. Rather, the observations are consistent with models that involve near-instantaneous changes in a hydrothermal system and models that involve near-instantaneous changes of the stress level on faults or cracks (Table 2).

When evaluating these models, however, it is important to keep in mind that earthquakes are likely triggered by more than one physical process. The observation that triggered seismicity occurs in two spatial and temporal bursts at Yellowstone, the Long Valley region, and Mount Rainier suggests that two or more mechanisms may be operating on different time-scales at each center. Although models that rely on changes in a magma chamber cannot explain seismicity triggered during the mainshock wave train, they may explain the delayed swarms in volcanic areas (Table 2).

Although triggered seismicity has been observed in a range of tectonic settings, including deep subduction zones (Tibi *et al.*, 2003) and intraplate North America (Hough, 2001; Gomberg *et al.*, 2004), triggering may occur preferentially in areas that are known or are likely to be geothermally active (Hill *et al.*, 1993, 2002). Several lines of evidence suggest that in hydrothermally/volcanically active

Table 2
Possible Mechanisms for Triggering

	Events During Wave Train			Swarms Delayed by Hours to Days		
	A	G	M	A	G	M
Nonlinear friction (e.g., Gomberg <i>et al.</i> , 1998)	X	X	X			
Stress corrosion (e.g., Gomberg, 2001)	X	X	X			
Unclogging fractures (Brodsky <i>et al.</i> , 2003)	?	X	X	?	X	X
Advective overpressure (Linde <i>et al.</i> , 1994)						X
Rectified diffusion* (Brodsky <i>et al.</i> , 1998)		X	X		X	X
Sinking crystal plumes (Hill <i>et al.</i> , 2002)						X
Relaxing magma body (Hill <i>et al.</i> , 2002)						X

Table assumes that triggered earthquakes are not aftershocks of local events. If triggered earthquakes are aftershocks, nonlinear friction and stress corrosion can lead to delayed swarms. A, anywhere; G, geothermal systems; M, magmatically active area. X indicates that triggering can happen in this situation. ? indicates this mechanism could happen anywhere, but is more effective in a geothermal system.

*Note that Ichihara *et al.* (2003) have pointed out theoretical problems with rectified diffusion.

areas, such as the ones described in this study, earthquakes are triggered remotely by changes in hydrothermal systems: (1) Large earthquakes have long been known to affect water levels in wells thousands of kilometers from the epicenter (e.g., Coble, 1965; Roeloffs *et al.*, 2003); (2) changes in geyser activity at Yellowstone directly correlated with shallow triggered seismicity in the immediate vicinity of the geysers (Husen *et al.*, 2004); (3) the frequency threshold for dynamic triggering observed in the Long Valley caldera region is consistent with triggering mechanisms that involve the movement of pore fluids (Brodsky and Prejean, 2003).

Investigating the tectonic regimes where triggered seismicity occurs may also help us to identify the triggering mechanism(s). To date, all the triggered earthquakes in geothermal and volcanic regions have occurred in extensional or transtensional environments (e.g., Brodsky *et al.*, 2000; Hill *et al.*, 2002; Moran *et al.*, 2004). In extensional and transtensional tectonic environments, Anderson faulting theory predicts that the cracks most likely to open would be oriented vertically. If seismic waves from large distant earthquakes change the hydrothermal system such that fluids can move upward along vertical fractures, then high-pressure fluids from depth would be rising to areas of the crust with lower pore pressure, possibly triggering earthquakes. Also, as discussed by Hough and Kanamori (2002), faults in extensional environments are expected to be relatively weak. It is thus possible that fractures will be opened by relatively low-stress changes in these environments, leading directly to unstable rupture.

Conclusions

Seismic waves from the M_w 7.9 Denali fault earthquake induced dynamic triggering of earthquakes across western North America at distances of at least 3660 km. This is the most distant case of remotely triggered seismicity yet observed. Because of recent improvements in seismic monitoring and increased awareness of remotely triggered seismicity, this and companion articles (Husen *et al.*, 2004; Moran *et al.*, 2004; Husker and Brodsky, 2004; Johnston *et al.*, 2004; Pankow *et al.*, 2004; Gomberg *et al.*, 2004) provide the most complete record of dynamically triggered seismicity ever documented for a single earthquake. The results of this study, however, highlight important observational challenges associated with the identification of remotely triggered earthquakes. Most notably, such events can escape detection when only standard processing and detection algorithms are used, even with a dense network of high dynamic-range seismometers.

At all the sites discussed in this article, the onset of triggered seismicity began during the Love and Raleigh waves with periods of 15 to 40 sec and peak dynamic stresses of 0.01–0.09 MPa. Earthquakes triggered during, and minutes after, the passage of surface waves from the M_w 7.9 were characterized by spasmodic bursts of small ($M < 2$), brittle-failure earthquakes. Swarms persisted for just a few minutes at Mount Rainier, 15–20 min at Mammoth Mountain in the Long Valley caldera and at Coso, and roughly 40 min at the Geysers.

As observed in previous studies, the areas that displayed the most vigorous swarms of remotely triggered seismicity, particularly during the wave train, were areas with active geothermal systems. A likely physical model to explain seismicity triggered during the Denali fault earthquake wave train in these areas involves changes in an area's hydrothermal system resulting from a relatively long period of ground shaking (e.g. Brodsky *et al.*, 2003; Brodsky and Prejean, 2003). Yellowstone, Mount Rainier, and the Long Valley caldera also responded to the Denali fault earthquake with bursts of triggered seismicity that were delayed by hours to days and were more energetic than the seismicity triggered during passage of the M_w 7.9 surface waves. This suggests that more than one mechanism generates remotely triggered earthquakes.

In the wake of the Denali fault earthquake, there are still many unresolved questions regarding the physical processes that drive remotely triggered seismicity. One question that remains is how the strain transients observed in Long Valley are related to triggered seismicity (Johnston *et al.*, 2004). We do not know whether such ground deformation is unique to Long Valley or if it is universal and has only been observed at Long Valley because it is the only site that is instrumented with borehole strain meters. Is ground deformation an integral part of the triggering response to large, distant earthquakes? If so, what does this imply for triggering processes?

The Denali fault earthquake has given us some leverage in interpreting the causative processes of remotely triggered seismicity. We have now observed repeated episodes of remote triggering at several sites, including the Geysers, Coso, and Long Valley. We also have detailed records of the spatio-temporal evolution of triggered earthquakes and associated local strain throughout the wave train of the Denali fault earthquake. These new and growing data sets provide an opportunity to test proposed triggering mechanisms and to better understand the physical process that leads to earthquake failure in general.

Acknowledgments

We thank Calpine Corp. of the Geysers geothermal field and the U.S. Navy Geothermal Program Office of the Coso geothermal field for providing data for this study. We thank Mitch Stark and Bob Sullivan for their assistance in conducting the research and Seth Moran, John Power, and Joan Gomberg for helpful reviews.

References

- Anderson, J. G., J. N. Brune, J. N. Louie, Y. Zeng, M. Savage, G. Yu, Q. Chen, and D. dePolo (1994). Seismicity in the western Great Basin apparently triggered by the Landers, California, earthquake, 28 June 1992, *Bull. Seism. Soc. Am.* **84**, 863–891.
- Bailey, R. (1989) Geologic map of the Long Valley caldera, Mono-Inyo craters volcanic chain, and vicinity, eastern California, *U.S. Geol. Surv. Misc. Inv. Ser.* 0160–0753.
- Brodsky, E. E., and S. G. Prejean (2003). Frequency dependent dynamic triggering, *EOS Trans. Am. Geophys. Un.* **84**, Abstract S31G-05.
- Brodsky, E. E., V. Karakostas, and H. Kanamori (2000). A new observation of dynamically triggered regional seismicity: earthquakes in Greece following the August, 1999 Izmit, Turkey, earthquake, *Geophys. Res. Lett.* **27**, 2741–2744.
- Brodsky, E. E., E. Roeloffs, D. Woodcock, I. Gall, and M. Manga (2003). A mechanism for sustained groundwater pressure changes induced by distant earthquakes, *J. Geophys. Res.* **108**, doi 10.1029/2002JB002321.
- Brodsky, E. E., B. Sturtevant, and H. Kanamori (1998). Volcanoes, earthquakes and rectified diffusion, *J. Geophys. Res.* **103**, 23,827–23,838.
- Coble, R. (1965). The effects of the Alaskan earthquake of March 27, 1964, on ground water in Iowa, *Iowa Acad. Sci.* **72**, 323–332.
- Eberhart-Phillips, D., P. J. Haeussler, J. T. Freymueller, A. D. Frankel, C. M. Rubin, P. Craw, N. A. Ratchkovski, G. Anderson, A. J. Crone, T. E. Dawson, H. Fletcher, R. Hansen, E. L. Harp, R. A. Harris, D. P. Hill, S. Hreinsdóttir, R. W. Jibson, L. M. Jones, D. K. Keefer, C. F. Larsen, S. C. Moran, S. F. Personius, G. Plafker, B. Sherrod, K. Sieh, and W. K. Wallace (2003). The 2002 Denali fault earthquake, Alaska: a large magnitude, slip-partitioned event, *Science* **300**, 1113–1118.
- Giampiccolo, E., C. Musumeci, S. D. Malone, S. Gresta, and E. Privitera (1999). Seismicity and stress-tensor inversion in the central Washington Cascade mountains, *Bull. Seism. Soc. Am.* **89**, 811–821.
- Glowacka, E., F. A. Nava, G. D. de Cossio, V. Wong, and F. Farafan (2002). Fault slip, seismicity, and deformation in Mexicali Valley, Baja California, Mexico, after the M 7.1 1999 Hector Mine earthquake, *Bull. Seism. Soc. Am.* **92**, 1290–1299.
- Gomberg, J. (2001). The failure of earthquake failure models, *J. Geophys. Res.* **106**, 16,253–16,263.
- Gomberg, J., and S. Davis (1996). Stress/strain changes and triggered seismicity at the Geysers, California, *J. Geophys. Res.* **101**, 733–749.
- Gomberg, J., N. M. Beeler, M. L. Blanpied, and P. Bodin (1998). Earth-

- quake triggering by transient and static deformation, *J. Geophys. Res.* **103**, 24,411–24,426.
- Gomberg, J., P. Bodin, K. Larson, and H. Dragert (2004). Earthquakes nucleated by transient deformations caused by the $M = 7.9$ Denali, Alaska, earthquake, *Nature* **427**, 621–624.
- Gomberg, J., P. Bodin, and P. A. Reasenberg (2003). Observing earthquakes triggered in the near field by dynamic deformations, *Bull. Seism. Soc. Am.* **93**, 118–138.
- Gomberg, J., P. A. Reasenberg, P. Bodin, and R. A. Harris (2001). Earthquake triggering by seismic waves following the Landers and Hector Mine earthquakes, *Nature* **411**, 462–465.
- Hill, D. P., W. L. Ellsworth, M. J. S. Johnston, J. O. Langbein, D. H. Oppenheimer, A. M. Pitt, P. A. Reasenberg, M. L. Sorey, and S. R. McNutt (1990). The 1989 earthquake swarm beneath Mammoth Mountain, California: an initial look at the 4 May through 30 September activity, *Bull. Seism. Soc. Am.* **80**, 325–339.
- Hill, D. P., M. J. S. Johnston, and J. O. Langbein (1995). Response of Long Valley caldera to the $M_w = 7.3$ Landers, California, earthquake, *J. Geophys. Res.* **100**, 12,985–13,005.
- Hill, D. P., F. Pollitz, and C. Newhall (2002). Earthquake-volcano interactions, *Phys. Today* **55**, 41–47.
- Hill, D. P., P. A. Reasenberg, A. Michael, W. J. Arabaz, G. Beroza, D. Brumbaugh, J. N. Brune, R. Castro, S. Davis, D. dePolo, W. L. Ellsworth, J. Gomberg, S. Harmsen, L. House, S. M. Jackson, M. J. S. Johnston, L. Jones, R. Keller, S. Malone, L. Munguia, S. Nava, J. C. Pechmann, A. Sanford, R. W. Simpson, R. B. Smith, M. Stark, M. Stickney, A. Vidal, S. Walter, V. Wong, and J. Zollweg (1993). Seismicity remotely triggered by the magnitude 7.3 Landers, California, earthquake, *Science* **260**, 1617–1622.
- Hough, S. E. (2001). Triggered earthquakes and the 1811–1812 New Madrid, central United States, earthquake sequence, *Bull. Seism. Soc. Am.* **91**, 1574–1581.
- Hough, S. E., and H. Kanamori (2002). Source properties of earthquakes near the Salton Sea triggered by the 16 October 1999 M 7.1 Hector Mine, California, earthquake, *Bull. Seism. Soc. Am.* **92**, 1281–1289.
- Husen, S., S. Wiemer, and R. B. Smith (2004). Remotely triggered seismicity in the Yellowstone National Park region by the 2002 $M_w = 7.9$ Denali Fault earthquake, Alaska, *Bull. Seism. Soc. Am.* **94**, no. 6B, S317–S331.
- Husker, A., and E. Brodsky (2004). Seismicity in Idaho and Montana triggered by the Denali fault earthquake: a window into the geological context for seismic triggering, *Bull. Seism. Soc. Am.* **94**, no. 6B, S310–S316.
- Ichihara, M., E. Brodsky, and H. Kanamori (2003). Reconsideration of the effect of rectified diffusion in volcanic-seismic systems (abstract), *Inter. Union Geophys. Geodesy Symposium*, Sapporo, Japan, July 2003.
- Johnston, M. J. S., S. G. Prejean, and D. P. Hill (2004). Triggered deformation and seismic activity under Mammoth Mountain in Long Valley Caldera by the November 3, 2002, M_w 7.9 Denali Fault earthquake, *Bull. Seism. Soc. Am.* **94**, no. 6B, S310–S316.
- Linde, A. T., I. S. Sacks, M. J. S. Johnston, D. P. Hill, and R. G. Bilham (1994). Increasing pressure from rising bubbles as a mechanism for remotely triggered seismicity, *Nature* **371**, 408–410.
- Mathews, M. V., and P. A. Reasenberg (1988). Statistical methods for investigating quiescence and other temporal seismicity patterns, *Pure Appl. Geophys.* **126**, 357–372.
- Moran, S. C., J. A. Power, S. D. Stihler, J. J. Sanchez, and J. Caplan-Auerbach (2004). Earthquake triggering at Alaskan volcanoes following the November 3, 2002, Denali Fault, earthquake, *Bull. Seism. Soc. Am.* **94**, no. 6B, S300–S309.
- Moran, S. C., D. R. Zimbelman, and S. D. Malone (2000). A model for the magmatic-hydrothermal system at Mount Rainier, Washington, from seismic and geochemical observations, *Bull. Volcanol.* **61**, 425–436.
- Pankow, K. L., W. J. Abarasz, J. C. Pechmann, and S. J. Nava (2004). Triggered seismicity in Utah from the November 3, 2002, Denali fault earthquake, *Bull. Seim. Soc. Am.* **94**, no. 6B, S332–S347.
- Power, J. A., S. C. Moran, S. R. McNutt, S. D. Stihler, and J. J. Sanchez (2001). Seismic response of the Katmai volcanoes to the 6 December 1999 magnitude 7.0 Karluk Lake earthquake, Alaska, *Bull. Seism. Soc. Am.* **91**, 57–63.
- Roeloffs, E., M. Sneed, D. L. Galloway, M. L. Sorey, C. D. Farrar, J. F. Howle, and J. Hughes (2003). Water-level changes induced by local and distant earthquakes at Long Valley caldera, California, *J. Vol. Geotherm. Res.* **127**, 269–303.
- Stark, M. A., and S. D. Davis (1996). Remotely triggered microearthquakes at The Geysers geothermal field, California, *Geophys. Res. Lett.* **23**, 945–948.
- Tibi, R., D. A. Wiens, and H. Inoue (2003). Remote triggering of deep earthquakes in the 2002 Tonga sequences, *Nature* **424**, 921–925.
- Unruh, J. R., E. Hauksson, F. C. Monastero, R. J. Twiss, and J. C. Lewis (2002). Seismotectonics of the Coso Range–Indian Wells Valley region, California: transtensional deformation along the southeastern margin of the Sierran microplate, *Geol. Soc. Am. Memoir*, Vol. 195, 277–294.
- Voisin, C. (2002). Dynamic triggering of earthquakes: the nonlinear slip-dependent friction case, *J. Geophys. Res.* **107**, 10–1–10–11.
- Waldhauser, F., and W. L. Ellsworth (2000). A double-difference earthquake location algorithm: Method and application to the northern Hayward fault, California, *Bull. Seism. Soc. Am.* **90**, 1353–1368.
- Weaver, C. S., and D. P. Hill (1978/79). Earthquake swarms and local crustal spreading along major strike-slip faults in California, *Pure Appl. Geophys.* **117**, 51–64.
- U.S. Geological Survey Alaska Volcano Observatory
Anchorage, Alaska 99508
(S.G.P.)
- U.S. Geological Survey
Menlo Park, California 94025
(D.P.H., M.J.S.J., D.H.O., A.M.P.)
- University of California, Los Angeles
Department of Earth and Space Sciences
Los Angeles, California 90095
(E.E.B.)
- U.S. Geological Survey
Pasadena, California 91106
(S.E.H.)
- University of Washington
Department of Earth and Space Sciences
Seattle, Washington 98195
(S.D.M.)
- U.S. Navy Geothermal Program
China Lake, California 93555
(K.B.R.)